Effect of annealing temperature and γ-irradiation on the electrical conductivity of stacked naphthalocyanine (SnNc - VoNc) thin films

NISHA S. PANICKER[1], JOSMI JOHN[2], I. REJEENA[3], C. S. MENON[4], R. L. THOMAS[5], VINOY THOMAS[2,*]
[1]*Department of Physics, KSM DB College, Sasthamcotta-690521, University of Kerala, India*
[2]*Center for Functional Materials, Department of Physics, Christian College Chengannur-689122, University of Kerala, India*
[3]*Department of Physics, MSM College Kayamkulam-686560, India*
[4]*School of Pure and Applied Physics, Mahatma Gandhi University, Kottayam -686560, India*
[5]*Department of Physics, St. Joseph's College for Women, Alappuzha-688001, University of Kerala, India*

Composite thin films of Tin (II) 2,3-naphthalocyanine (SnNc) and Vanadyl 2,3-naphthalocyanine (VoNc) were prepared by the novel stacked vacuum deposition techniques. In order to study the effect of defect induced conductivity of these films, the prepared films are subjected to heat treatment and γ-ray irradiation. Surface morphological features are investigated using Scanning electron microscopy (SEM) and observed that this technique yields continuous films without any segregation. UV-Vis-NIR spectrum shows a characteristics of broad Q-band spectrum for composite thin films. The electrical conductivity studies of stacked films for various heat treatment stages and γ-ray irradiation shows better conductivity compared to other naphthalocyanine counterpart and the activation energy is found to increase with annealing temperature.

(Received February 6, 2024; accepted December 2, 2024)

Keywords: Organic semi-conductors, Naphthalocyanines, Electrical conductivity, Annealing, Gamma irradiation

1. Introduction

In recent years, phthalocyanines and naphthalocyanines have garnered significant interest in various fields such as materials science, medicine, catalysis, display technologies, cutting-edge technological applications etc [1-4]. The phthalocyanines (Pc) and naphthalocyanines (Nc) are basically formed with macrocycle prototypes for the formation of molecular crystals and cofacially linked polymers which can attain high electrical conductivities [5-6]. In these materials the charge carriers belong to the π-molecular orbitals of the macrocycle whose mobility depends on the extension of overlap between two adjacent macrocycles. In our previous studies we have demonstrated the production of thermally evaporated, vacuum deposited, single component thin films of tin and vanadyl naphthalocyanines. It was also shown that gamma ray irradiation and thermal annealing can bring about changes in the conductivities of Pc and Nc thin films due to the charge mobilization/distribution within the film matrix [7-8]. Radiation induced structural defects such as colour centres are usually formed when an electron becomes bound to a vacancy. It is reported that the density of colour centres increases when the films are exposed to gamma rays giving rise to changes in both optical and electrical properties [9-11].

The increasing prominence of phthalocyanines and naphthalocyanines is largely due to their versatility in forming thin-film transistors, light-emitting diodes, recordable media, Schottky diodes, and other key components in modern electronic devices [12-13]. In the current research scenario, the naphthalocyanine molecules joins the next generation single molecule electronic technology which is accomplished through its intrinsic hydrogen tautomerization property to serve as memory elements, diodes, transistors, or switches [14]. Despite the proven qualities of the extended π-electron molecules, there have been very few studies investigating their intrinsic or extrinsic properties as semiconductors [12-13,15]. Earlier reports investigating the conductivities of un-substituted and metal substituted naphthalocyanines showed better performance compared to its Pc counterparts. In this study, we investigate the electrical conductivity of composite thin films formed by Tin (II) 2,3-naphthalocyanine (SnNc) and Vanadyl 2,3-naphthalocyanine (VoNc) using a novel stacked coating technique via thermally evaporated vacuum deposition. This stacked coating technique enables precise layering of SnNc and VoNc thin films, leading to enhanced uniformity, continuity, and conductivity compared to traditional single-layer or co-deposited films. The films, with VoNc grown on SnNc (Sn-Vo) and SnNc grown on VoNc (Vo-Sn) configurations, exhibited significant improvements in conductivity after thermal annealing and gamma irradiation treatments. The impacts of these treatments on conductivity were systematically evaluated, highlighting the effectiveness of the deposition and post-treatment processes.

The stacked SnNc and VoNc thin films show promising potential for applications in ultra-high-density storage and photoconductive devices [16-17]. Additionally,

this composite material optimization could be instrumental in determining the optical semiconductor energy gaps essential for designing transparent solar cells using one, two, or three material layers [18-20]. The development of transparent solar cells is a prominent and timely area of research, aimed at increasing solar energy harvesting through solar cell windows for shops and homes, aligning with global efforts to reduce carbon emissions by 50%. This innovative approach in our study not only strengthens the optical and electrical properties of composite films but also opens new pathways for sustainable, carbon-reducing technologies in optoelectronics and energy solutions.

2. Materials and methods

The thin film deposition was carried out using a Hind Hivac vacuum coating unit model No. 12A4. A novel stacked coating technique was employed to grow thin films using two resistive heating terminals and two distinct molybdenum boats. At first VONc powder was sublimed to form thin film on the substrate, whose growth thickness was monitored. Eventually, using a manual shutter the VONc deposition was cut-off and current supply was switched to the second heater electrode to form SnNc thin film over the VONc film surface (VO-Sn stacked). As a separate experiment the coating sequence was reversed to grow VONc film over SnNc film (Sn-VO stacked). There is limited literature or research on the deposition of one organic film over another via thermally evaporated and vacuum deposited technique [21].

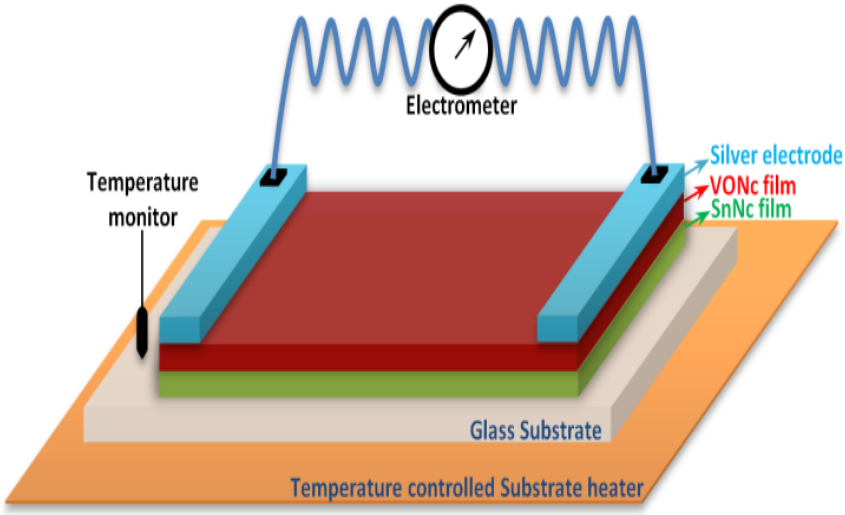

Fig. 1. The conductivity cell arrangement for deducing the activation energy of the stacked thin films (color online)

The thin films were γ-irradiated with a ^{60}Co gamma source at three different dosages, viz.195.8krad, 97.9krad and 48.9krad for 60 minutes. The electrical measurements were carried out using a programmable Keithley electrometer (model No.617) for all the samples. To avoid all possible contaminations, conductivity measurements were performed in a vacuum-sealed environment at 0.133Pa and in a dark chamber to minimize both atmospheric exposure and the photoconductive contribution of the molecules. In situ measurements were not used, but the transfer was carefully controlled to maintain sample integrity during the process. A representative diagram of the conductivity measurement setup is shown in Fig. 1. The films were also annealed at four different annealing stages viz. 300K (as-deposited), 323K, 373K, 423K and 473K.

3. Results and discussions

3.1. Surface morphological studies

The structural characterization of the thin films was carried out using scanning electron microscopy (SEM). Energy dispersive X-ray analysis (EDX) was employed to confirm and identify the growth of the SnNc and VoNc films. The as-deposited Vo-Sn stacked thin film exhibits a uniform distribution of SnNc over the VoNc layer (Fig. 2). The morphology of the composite thin film appears even and continuous, with sub-micron particles present. This improved uniformity is expected to result in higher optical quality and transparency compared to single-layer films or mixed films, where SnNc and VoNc are co-deposited simultaneously in a single layer. Higher resolution scale of as-deposited films of VO-Sn stacked (Fig. 2-inset) showed some kind of blister like growth. This eventually disappeared at higher heat treatment stage (Supporting document 1) which shows spherical particle morphology. On gamma irradiation up to 195.8krad (Supporting Fig. 2), the film seems to have evident sub-microcrystalline

morphology, whose growth (Supporting figure) might have been induced by the irradiation with Compton electrons.

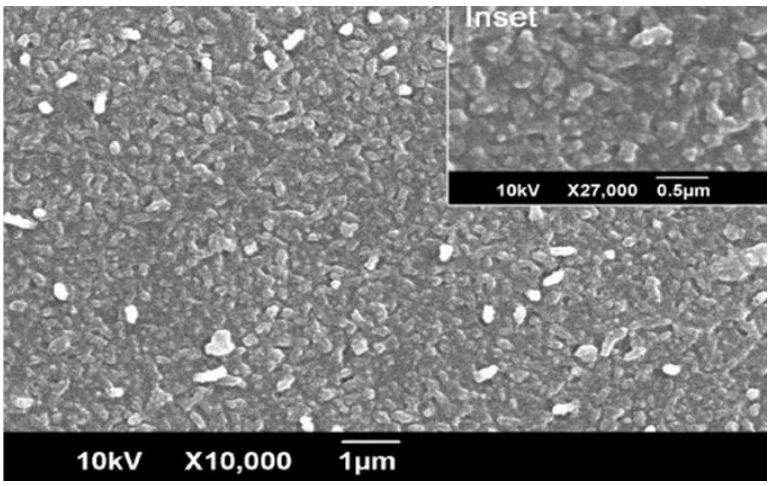

Fig. 2. SEM image of as-deposited VO-Sn stacked thin film. Inset – 500nm resolution scale

The as-deposited Sn-VO stacked thin film shows a different morphology revealing its highly porous structures with elongated particles (Fig. 3). On heat treatment to 373K (Fig. 3- inset) the porosity is still maintained but the particles become more uniform in shape. A new observation was brought to light on heat treatment to 473K (Supporting document 3) the film microstructure entirely changes with a prominent blister like growth on the larger particles and the porosity of the film is enhanced very much. On gamma irradiation, the blister growth seen at higher heat treatment is replicated, though the film remains non-porous (Supporting document 4). The results and observations from the SEM analysis for various films at different treatment stages have been consolidated and presented in Table 1.

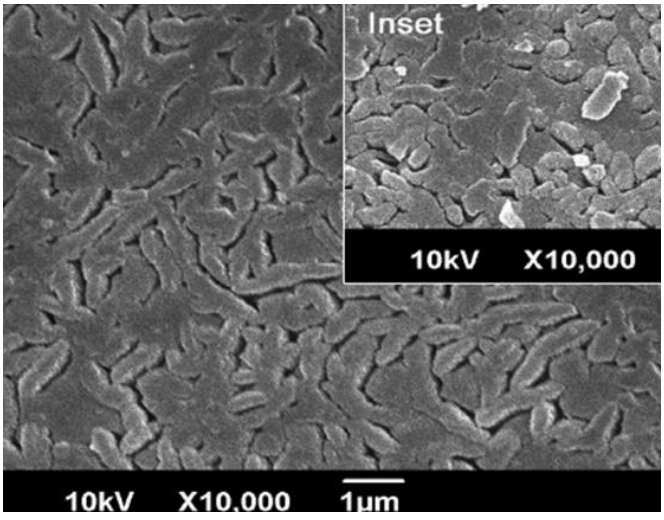

Fig. 3. SEM image of as-deposited Sn-VO stacked thin film. Inset- annealed to 373K

Table 1. SEM morphological comparison of various thin films

Sample	As-deposited	373K heat treatment	473K heat treatment	195.8krad γ-irradiation
Mixed	Cohabitated growth of both components, grainy and continuous			
VO-Sn	Particles with small blisters, continuous	Particles, blisters disappear, continuous		Sub-micro crystal lumps
Sn-VO	Elongated particles, porous	Spherical particles, porous	Blisters appear and high porosity	Large blisters with almost no porosity

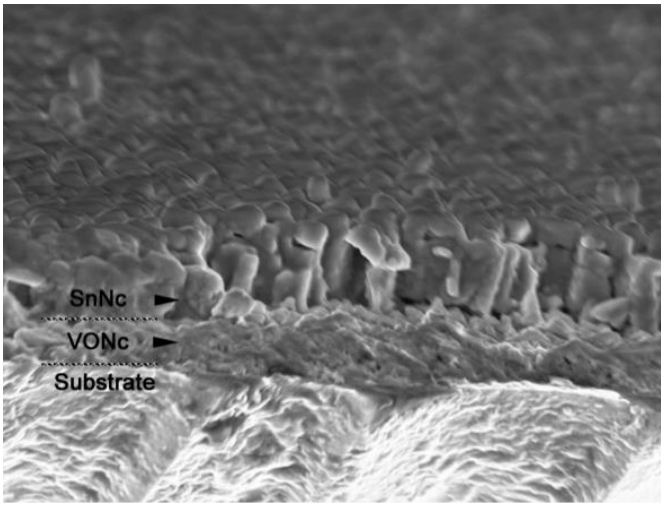

Fig. 4. SEM image of cross-section of as-deposited VO-Sn stacked thin film

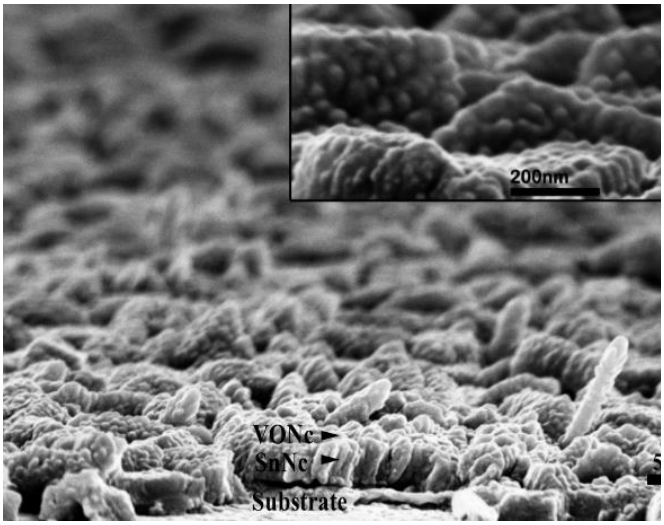

Fig. 5. SEM image of cross-section of as-deposited Sn-VO stacked thin film. Inset-200nm resolution scale

A cross-sectional view of all the samples was taken to observe the growth pattern. Fig. 4 and Fig.5 shows the cross section of VO-Sn stacked and Sn-VO stacked samples respectively. The interface between the substrate and two molecular films are clearly seen distinguished in the SEM of VO-Sn stacked. The SEM images clearly indicate that the film growth is continuous without any substantial segregation due to cohabitation of two different naphthalocyanine compounds. Fig. 5 shows a perfect film growth of one over the other, the debris and the irregular facet is due to the bad end-facet cleaving, great deal of care was taken to reduce any kind of stress being transferred to the film while cleaving. The cross-sectional SEM image of the Sn-VO stacked film provided new insights into blister formation. These blister-like structures are basically due to the VONc layer growing directly on the SnNc layer as a cohesive unit, with no visible separation between the layers.

3.2. The UV-Vis-NIR absorption studies

The UV-Vis-NIR absorption measurements for Sn-VO and VO-Sn stacked thin films are shown in Fig. 6. Both stacked samples showed signature peaks almost identical for as-deposited and gamma irradiation stages, indicating high stability of the films against heat treatment and high-energy radiation. The Q-band (700-950nm) peak for vacuum deposited VONc and SnNc were reported to be around 814nm and 845nm respectively [7-8,22]. A composite thin film using these two materials could produce a broad Q-band spectrum. VO-Sn stacked samples showed higher oscillator strength compared to Sn-VO stacked samples. It was found that on annealing to 473K, both stacked samples showed broadening in the Q-band and a red shift in Q-band peaks shifting to 860nm. Since the Q band is sensitive to the environment of the Pc or Nc molecule, a broad Q band spectrum for stacked film ensures a uniform SnNc film growth over VONc [22-23]. The shifting of peaks is attributed to the formation of dimeric species upon annealing. It was previously observed that gamma irradiation on single VONc samples induced a huge production of dimeric species. But this situation was avoided to a great extend in the mixed samples.

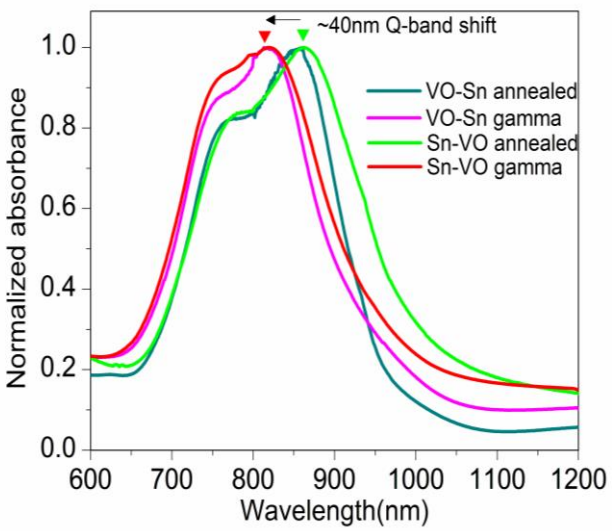

Fig. 6. Q band spectra of VO-Sn and Sn-VO sampled in their annealed and gamma irradiated states (color online)

3.3. Electrical conductivity studies

The electrical conductivity of the organic semiconductor obeys the Arrhenius equation, the electrical conductivity σ can be expressed as:[24]

$$\sigma = \sigma_0 exp\left(\frac{-E}{k_b T}\right)$$

σ is the conductivity at temperature T, E is the thermal activation energy, k_B is the Boltzmann constant and σ_0 is the pre-exponential factor. The thermal activation energy, which is the minimum energy required to liberate charge

carriers from traps or ionization levels within the band gap, is calculated from the slope of lnσ vs 1000/T.

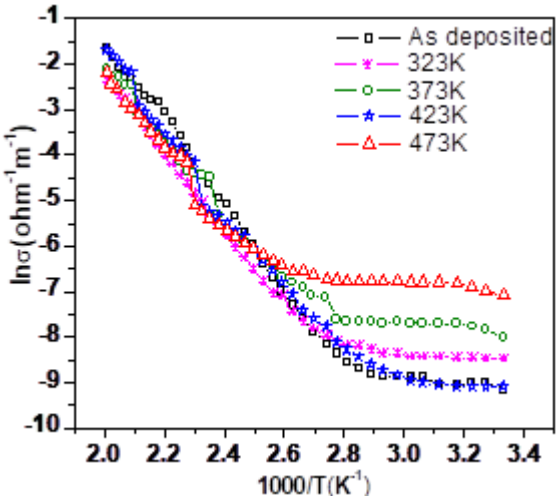

Fig. 7. lnσ vs 1000/T plot for VO-Sn stacked samples as-deposited and annealed from 323K to 473K (color online)

The electrical conductivity of VONc grown on SnNc (Sn –VO stack) as a function of temperature is given in Fig. 7 for as-deposited and annealed films. The conductivity values for as-deposited and annealed samples follows the same trend of their single precursors as reported in our earlier works. The activation energies calculated for as-deposited, annealed and γ-ray irradiated samples are given in the Table 2. Form the table it is clear that only two activation energies exist for as-deposited and samples annealed at low temperature (323K). It indicates that the conductivity depends mainly on the electron-hole production via thermal transition from a valence band to the conduction band [25]. For samples annealed above 323K, the three-step curve indicates the contribution of extrinsic conductivity due to the defect states near the band edge [26]. The activation energy decreases with increase in annealing temperature. There was a remarkable increase in conductivity values with a very low activation energy values for moderate or high temperature conductivity measurements. Since the film matrix is formed of two different materials, a heat treatment could produce pseudo-Fermi levels enhancing the charge mobility throughout the matrix [27].

Table 2. Activation energies E_1, E_2, E_3 obtained for 2annealed and γ-irradiated Sn-VO samples

Annealed/γ-irradiated sample	Activation energy (eV)		
	E1	E2	E3
300K	-	0.75	0.07
323K	-	0.74	0.02
373K	0.64	0.69	0.04
423K	0.44	0.68	0.05
473K	0.29	0.32	0.02
48.9krad	-	0.64	0.21
97.9krad	0.74	0.63	0.11
195.8krad	0.23	0.47	0.03

Fig. 8 shows the effect of γ-ray irradiation for VO-Sn stacked samples. The conductivity curves remain same as that of VONc or SnNC thin films. But upon irradiation with a dosage of 195.8krad, there was a remarkable increase in conductivity values with a very low activation energy values for moderate or high temperature conductivity measurements. In comparison with the annealed or other gamma irradiation stages of the sample, 195.8krad irradiated samples showed more abrupt breaks in the curves which is a manifested indication of thermal excitation of defect states that lies near the band edge, contributing towards the conduction [28]. The production of such defect states was induced by strong gamma irradiation and was also evident from the changes in its surface morphology. The thermal annealing and γ-ray irradiation also produce same results on VO-Sn stacks but with lower activation energy values.

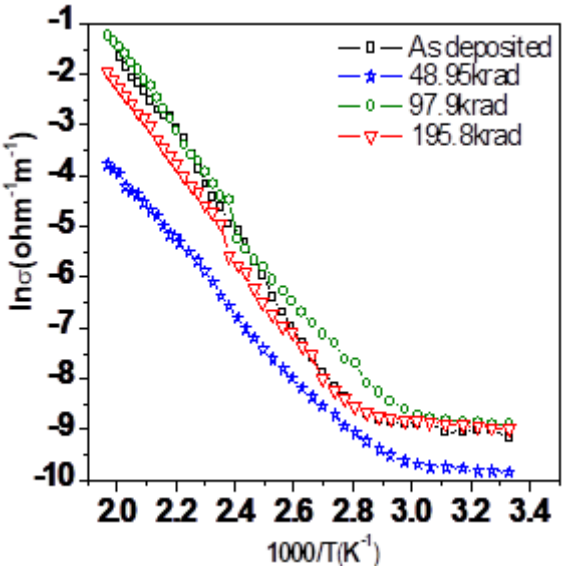

Fig. 8. lnσ vs 1000/T graph for VO-Sn stacked samples γ-irradiated at 48.9 krad, 97.9 krad and 195.8 krad (color online)

On detailed analysis of both stacked depositions, it appears that high conductivity is influenced not only by the mutual presence of VONc and SnNc but also by the specific sequence in which they are deposited. This is evident from the uniform nanoparticle structures observed in Sn-VO stacked films (Fig. 3), which may result from a nucleation process triggered by gamma irradiation and favourable growth conditions. A similar nucleation process was also observed in Sn-VO stacked films annealed at 473K, although only a slight enhancement occurred, likely due to the high porosity present in the material. As per our speculation, the substantial reorientation of the Q-band in the absorption spectra played a key role in enhancing conductivity. An evident blue shift in the Q-band effectively reduced the band-gap as well. This reduction can likely be attributed to an increase in radiation-induced structural defects, which may expand the localized and extended states, thereby creating a narrower energy band gap [28] and subsequently lowering the values at the absorption edge. An in-depth examination of potential

migration of SnNc and VONc species, along with the formation of a pure-hybrid interconnection that could improve conductivity, is evident at this preliminary phase of the research.

4. Conclusions

Thin films of Tin (II) 2,3-naphthalocyanine (SnNc) and Vanadyl 2,3-naphthalocyanine (VoNc) are prepared using a novel stack deposition technique. The prepared films are analysed using SEM and UV-Vis-NIR absorption studies. Good quality thin films were obtained via these techniques. SEM images shows that these thin films would be quite stable on thermal annealing and gamma irradiation dosages. Stacked thin film showed a particulate and sub-microcrystalline morphology on heat treatment and gamma irradiation. The optical absorption measurements showed a broad Q-band spectra centered around 820-860nm. The higher oscillating strength of Q-band shows that these films can be used as suitable absorber to attain the desired values for Q-Switching and mode-locking to obtain short and ultrafast laser pulses of nanosecond and pico-second durations. Regarding the conductivity of the thin films, when VONc was grown on SnNc film, a maximum gamma irradiation produced the best ever reported results for SnNc or VONc thin films. The conductivity values rose several times higher significantly with a very low activation energy over a range from 300K-500K measurement range which might be due to the production of large number of defect states that lies near the band edge.

Acknowledgements

R. L. Thomas is grateful to Department of science and Technology (Govt of India) for research support (DST/CURIE-PG/2023/9).

References

[1] M Urbani, G. de la Torre, M. K. Nazeeruddin, T. Torres, Chem. Soc. Rev. **48**, 2738 (2019).
[2] N. M. Kuprikova, D. D Klyamer, A. S Sukhikh, P. O. Krasnov, I. Mrsic, T. V. Basova, Dyes and Pigments **173**, 107939 (2020).
[3] H. A. R. Aliabad, M. Bashi, J. Mater. Sci. Mater. Electron. **30**, 18720 (2019).
[4] N. R. da Silva Gobo, T. J Brocksom, K. T. de Oliveira, Molecules **25**(9), 2164 (2020).
[5] C. G. Claessens, U. Hahn, T. Torres, Chemical Record **8**, 75 (2008).
[6] J. S. Prauzner-Bechcicki, S. Godlewski, M. Szymonski, Physica Status Solidi A **209**(4), 603 (2012).
[7] N. S. Panicker, C. S. Menon, Journal of Materials Science **46**, 4479 (2011).
[8] N. S. Panicker, T. G. Gopinathan, I. Dhanya, C. S. Menon, Physica B: Condensed Matter **40**, 54556 (2010).
[9] E. A. B. Silva, J. F. Borin, P. Nicolucci, C. F. O. Graeff, T. G. Netto, R. F. Bianchi, Applied Physics Letters **86**, 131902 (2005).
[10] M. M. El-Nahass, A. A. M. Farag, A. A. Atta, Synthetic Metals **159**, 589 (2009).
[11] J. Barichello, P. Mariani, L. Vesce, D. Spadaro, I. Citro, F. Matteocci, A. Bartolotta, A. Di Carlo, G. Calogero, Journal of Materials Chemistry C **12**, 2317 (2024).
[12] W. H. Flora, H. K. Hall, N. R. Armstrong, Journal of Physical Chemistry B **107**, 1142 (2003).
[13] L. Talazac, F. Barbarin, C. Varenne, L. Mazet, S. Pellier, S. Soulier, Sensors and Actuators B **83**, 149 (2002).
[14] E. Orti, R. Crespo, M. C Piqueras, J. L. Bredas, Synthetic Metals **41-43**, 2647 (1991).
[15] T. Tomiyama, I. Watanabe, A. Kuwano, M. Habiro, N. Takane, M. Yamada, Applied Optics **34**, 8201 (1995).
[16] A. M Hassanien, A. A. Darwish, A. M. Kamal, Physica Scripta **99**, 055532 (2024).
[17] W. Zhou, N. J. Yutronkie, B. H. Lessard, J. L. Brusso, Advanced Materials **2**, 165 (2021).
[18] A. Suzuki, N. Ohashi, T. Oku, T. Tachikawa, T. Hasegawa, S. Fukunishi, Journal of Electronic Materials **53**, 6049 (2024).
[19] G. H. Al-Hazmi, A. M. Hassanien, A. A. Atta, M. S. Refat, H. A. Saad, S. Shakya., A. M. A. Adam, Journal of Molecular Liquids **362**, 119757 (2022).
[20] Q. Lv, R. Yu, R. Shi, Z. Tan, Materials Chemistry Frontiers **7**, 5063 (2023).
[21] Z. He, G. Zhao, G. Han, Physica Status Solidi A **203**, 518 (2006).
[22] H. Yanagi, M. Ashida, J. Elbe, D. Wohrle, The Journal of Physical Chemistry **94**, 7056 (1990).
[23] B. Wang, X. Zuo, X. Cheng, Y. Wu, Thin Solid Films **517**, 937 (2008).
[24] D. D. Eley, G. D. Parfitt, Transactions of the Faraday Society **51**, 1529 (1955).
[25] S. Tai, N. Hayashi, Journal of the Chemical Society-Perkin Transactions **2**, 1275 (1991).
[26] M. M. El-Nahass, A. A. M. Farag, A. A. Atta, Synthetic Metals **159**, 589 (2009).
[27] N. F. Mott, E. A. Davis, The Philosophical Magazine **22**, 903 (1970).
[28] M. M. El-Nahass, A. A. M. Farag, A. A. Atta, Synthetic Metals **159**, 589 (2009).

*Corresponding author: vinoythoma@gmail.com